

Superradiant Instability and Backreaction of Massive Vector Fields around Kerr Black Holes

William E. East¹ and Frans Pretorius²

¹*Perimeter Institute for Theoretical Physics, Waterloo, Ontario N2L 2Y5, Canada and*

²*Department of Physics, Princeton University, Princeton, New Jersey 08544, USA*

We study the growth and saturation of the superradiant instability of a complex, massive vector (Proca) field as it extracts energy and angular momentum from a spinning black hole, using numerical solutions of the full Einstein-Proca equations. We concentrate on a rapidly spinning black hole ($a = 0.99$) and the dominant $m = 1$ azimuthal mode of the Proca field, with real and imaginary components of the field chosen to yield an axisymmetric stress-energy tensor and, hence, spacetime. We find that in excess of 9% of the black hole’s mass can be transferred into the field. In all cases studied, the superradiant instability smoothly saturates when the black hole’s horizon frequency decreases to match the frequency of the Proca cloud that spontaneously forms around the black hole.

Introduction.—A remarkable feature of spinning black holes (BHs) is that a portion of their mass—up to 29% for extremal spin—can, in principle, be extracted. One way to realize this liberation of rotational energy is through the interaction of the BH with an impinging wave—be it scalar, electromagnetic, or gravitational—with frequency $\omega < m\Omega_{\text{BH}}$, where Ω_{BH} is the BH horizon frequency and m is the azimuthal number of the wave. Waves satisfying this criterion exhibit superradiance and carry away energy and angular momentum from the BH. An analogous phenomenon can occur for charged BHs, where the electromagnetic energy of the BH is superradiantly transferred to an interacting charged matter field interacting with the BH.

Going back to Ref. [1], there has been speculation of how superradiance could be combined with a confining mechanism to force the wave to continuously interact with the BH and hence undergo exponential growth—a so called “black hole bomb.” The first nonlinear studies of this process were recently undertaken for a charged scalar field around a charged BH in spherical symmetry, both in a reflective cavity in asymptotically flat space [2], and in the naturally confining environment of an asymptotically anti-de Sitter domain [3].

However, there is an exciting possibility that a variation of this scenario could, in fact, be realized around astrophysical spinning BHs. Massive bosonic fields with a Compton wavelength comparable to, or larger than, the horizon radius of a BH can form bound states around the BH, and if the latter is spinning, the bound states can grow from a seed perturbation through superradiance [4–6]. This implies that stellar mass BHs can probe the existence of ultralight bosons

with masses $\lesssim 10^{-10}$ eV that are weakly coupled to ordinary matter and thus difficult to detect by other means. Theoretical scenarios where this might occur include the string axiverse [7, 8], the QCD axion [9], and dark photons [10, 11]. Such particles could form large clouds, spinning down the BH in the process. This is of particular interest now that LIGO has begun observing gravitational waves (GWs) [12], since measurements of BH masses and spins from binary mergers can be used to rule out or provide evidence for such particles, in addition to direct searches for the GW signatures of boson clouds [13, 14]. See [15] for a review.

Though details of the nonlinear growth and saturation of the rotational superradiant instability will be important to help observe or rule out such massive fields, there are presently few results of relevance to this regime where the backreaction on the BH is significant. In Ref. [16], it was found that, for sufficiently large GWs superradiantly scattering off a Kerr BH, backreaction effects decrease the efficiency of energy extraction (for the analogous case of the scattering of a charged scalar field by a Reissner-Nordström BH, see [17]). The nonlinear behavior of the superradiant instability of massive bosons has not been addressed before. This is because of the computational cost of solving the equations, in part due to the disparate time scales between the oscillation of the field and the growth rate of the instability and the lack of symmetries to reduce it to a $(1+1)$ -dimensional problem (unlike the charged case). Important questions include what the efficiency of energy and angular momentum extraction is, how explosive the nonlinear phase of growth is (e.g., can the energy extraction overshoot limits implied by the parameters of the field

and BH [2]), and what the final state is after a non-negligible amount of energy has been transferred to the Proca field (e.g., does a stable cloud form around the BH, or could there be something akin to a *bosenova* where the entire field is rapidly expelled from the vicinity of the BH).

In this Letter we begin to address these questions related to the nonlinear behavior of the superradiant instability of massive bosonic fields around a spinning BH. We focus on the case of a vector field, as it exhibits faster growth than a scalar field. The linear regime of the instability for Proca fields has been studied before in various limits [11, 14, 18–20]. Here we find numerical solutions of the full Einstein-Proca field equations. To make the problem computationally tractable, we use a complex field with prescribed $m = 1$ azimuthal dependence to give an axisymmetric stress-energy tensor and, hence, spacetime geometry. Beginning with a seed field about a rapidly rotating BH, we find that the instability efficiently grows into the nonlinear regime and smoothly saturates when the BH horizon frequency decreases to match that of the Proca cloud. This frequency depends on the mass parameter of the field, and for a value near where we expect maximal energy extraction, we find that when the instability saturates a large Proca cloud has formed, containing 9% of the initial BH mass (and 38% its initial angular momentum). We use units with $G = c = 1$ throughout.

Methodology.—We consider a Kerr BH with initial mass M_0 and dimensionless spin $a = 0.99$ in the presence of a complex Proca field X^a with constant mass parameter μ , and numerically evolve the coupled Einstein-Proca equations. The Proca field equation of motion is $\nabla_a F^{ab} = \mu^2 X^b$, where $F_{ab} = \nabla_a X_b - \nabla_b X_a$, and its corresponding stress-energy tensor is

$$T_{ab} = \frac{1}{2}(F_{ac}\bar{F}_{bd} + \bar{F}_{ac}F_{bd})g^{cd} - \frac{1}{4}g_{ab}F_{cd}\bar{F}^{cd} + \frac{\mu^2}{2}(X_a\bar{X}_b + \bar{X}_aX_b - g_{ab}X_c\bar{X}^c), \quad (1)$$

where the overbar indicates complex conjugation. We evolve the Proca equations in a form similar to Ref. [21] (which also evolved the Einstein-Proca equations, though without symmetry restrictions and focusing on nonlinear interactions between the field and a nonspinning BH). We restrict to cases where the Proca field has an $m = 1$ azimuthal dependence and the resulting stress-energy tensor and spacetime are axisymmetric—i.e., in terms of the Lie derivative with respect to the axisymmetric Killing vector $(\partial/\partial\phi)^b$, $\mathcal{L}_\phi X_a = iX_a$. This allows us to use a two-dimensional

numerical domain for the spatial discretization, which is essential in making evolutions on time scales of $\sim 10^5 M_0$ computationally feasible. Here we study cases with $\tilde{\mu} := M_0\mu = 0.25, 0.3, 0.4,$ and 0.5 . As we discuss below, $\tilde{\mu} = 0.25$ is near the value that maximizes the energy extracted from the BH, while $\tilde{\mu} = 0.5$ is close to the value that gives the maximum growth rate for the linear instability [22]. We begin with a seed Proca field with energy $\sim 10^{-3}M_0$ around a Kerr BH (ignoring the effect of this small field on the initial spacetime geometry) and study the subsequent evolution. We have verified that using different or lower amplitude perturbations gives similar results.

We evolve the Einstein equations using the generalized harmonic formulation, with the gauge degrees of freedom set by fixing the source functions to the values of the initial BH solution in Kerr-Schild coordinates, as in Ref. [16]. To mitigate the accumulation of truncation error during the long period it takes for the Proca field to grow large enough to significantly backreact on the spacetime, we use the background error subtraction technique described in Ref. [23], with the initial isolated spinning BH as the background solution. As the spacetime evolves, we keep track of the BH apparent horizon and measure its area A and angular momentum J_{BH} , from which we can derive a mass using the Christodoulou formula

$$M_{\text{BH}} = \left(M_{\text{irr}}^2 + \frac{J_{\text{BH}}^2}{4M_{\text{irr}}^2} \right)^{1/2}, \quad (2)$$

where $M_{\text{irr}} = \sqrt{A/16\pi}$ is the irreducible mass. We also measure the flux of Proca field energy \dot{E}^H and angular momentum \dot{J}^H through the BH horizon. In addition, for the Proca field we keep track of the energy density $\rho_E = -\alpha T_t^t$ and angular momentum density $\rho_J = -\alpha T_\phi^t$ (where $\alpha = [-g^{tt}]^{-1/2}$ is the lapse), the volume integrals of which give a measure of the total energy E and angular momentum J outside of the BH horizon. Details on the numerical resolution and convergence are given in the appendix; more information on how we evolve the Proca equations, as well as results on the instability in the test-field regime, are provided in Ref. [22].

Results.—All the cases studied here are susceptible to a linear superradiant instability, and after a brief transient period the energy and angular momentum in the Proca field enter a period of exponential growth as shown in Fig. 1. As also shown there, the corresponding loss of mass and angular momentum by the BH, as measured from its horizon properties, closely tracks this. The cases with larger μ have larger growth

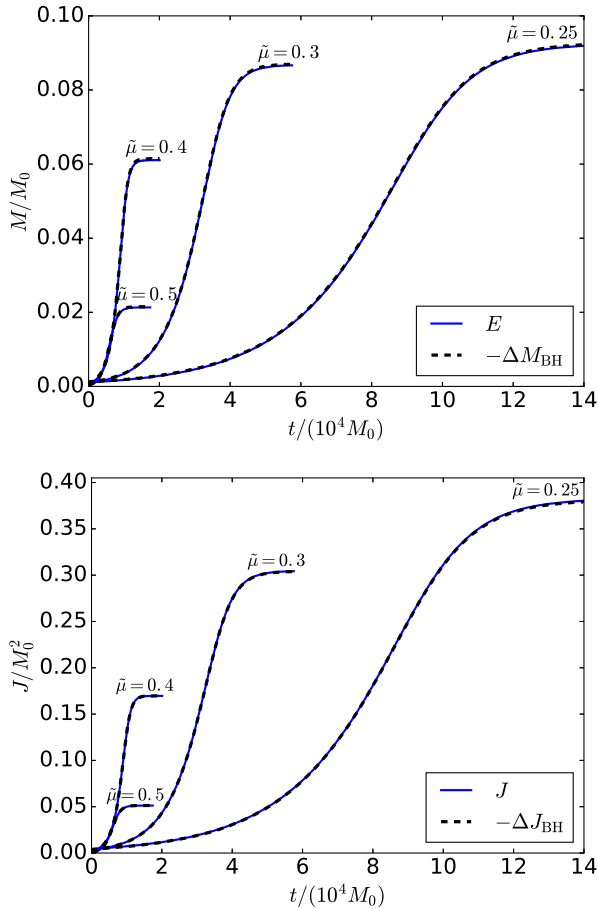


FIG. 1. The energy (top) and angular momentum (bottom) in the Proca field as a function of time (solid lines), along with the loss in mass (top) and angular momentum (bottom) of the BH (dashed lines).

rates for the instability and also saturate with smaller energy and angular momentum. Though the mass of the BH is decreasing in each case, as required by BH thermodynamics the irreducible mass M_{irr} is always increasing, and smaller μ cases saturate with a larger overall increase in M_{irr} .

The reason for the saturation of the superradiant instability is illustrated in Fig. 2, where we plot both the horizon frequency of the BH Ω_{BH} and the ratio of Proca field energy to angular momentum flux through the horizon \dot{E}^H/j^H . When $\Omega_{\text{BH}} > \dot{E}^H/j^H$, the superradiant condition is met and the Proca cloud will extract rotational energy from the BH. However, as shown in Fig. 2, eventually the BH’s horizon frequency decreases to the point where $\Omega_{\text{BH}} \approx \dot{E}^H/j^H$, and the

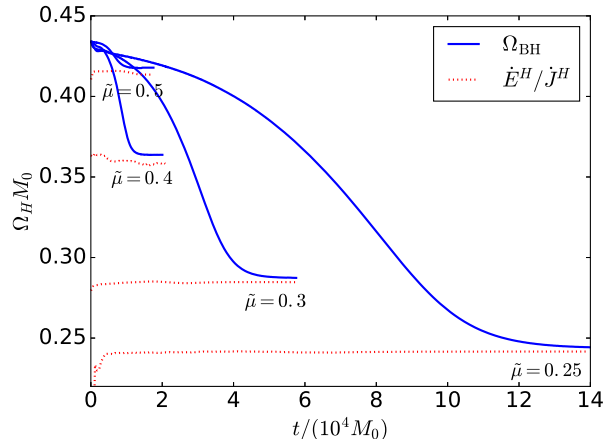


FIG. 2. The BH horizon frequency Ω_{BH} , as calculated from the BH’s mass and angular momentum, and the ratio of the flux of Proca field energy and angular momentum \dot{E}^H/j^H through the BH horizon, as a function of time.

instability saturates.

We can obtain simple estimates of the final state properties of the black hole if we assume, as roughly consistent with the simulations, that the instability will extract energy and angular momentum in some fixed proportion $\omega(\mu) = \dot{E}^H/j^H$ [where $\omega(\mu) \approx \mu(1 - \tilde{\mu}^2/2)$ in the linear/small $\tilde{\mu}$ limit [24, 25]] until $\omega(\mu) = \Omega_{\text{BH}}$. We plot the results in Fig. 3, along with the four end-state points from the full nonlinear simulations, showing excellent agreement with the approximation. This indicates an efficient extraction of energy and angular momentum, with a negligible additional increase in irreducible mass (equivalently, BH entropy). This is likely due to the relatively slow evolution of the instability compared to the light-crossing time of the BH, even approaching saturation (similar conclusions were reached using a “quasiadiabatic” approximation for the massive scalar field instability in Refs. [26, 27]). We see that the energy lost by the BH should be maximized at $-\Delta M_{\text{BH}}/M_0 \approx 0.093$, near the value $-\Delta M_{\text{BH}}/M_0 \approx 0.092$ found for $\tilde{\mu} = 0.25$ here. For lower values of μ , less energy, but more angular momentum will be extracted, with the instability just converting the Kerr BH into a nonspinning BH of the same mass in the $\mu \rightarrow 0$ limit.

After saturation, the resulting configuration consists of a BH surrounded by a Proca cloud with roughly stationary energy density, though the phase of the complex field is oscillating at a constant frequency. The energy and angular momentum density of the re-

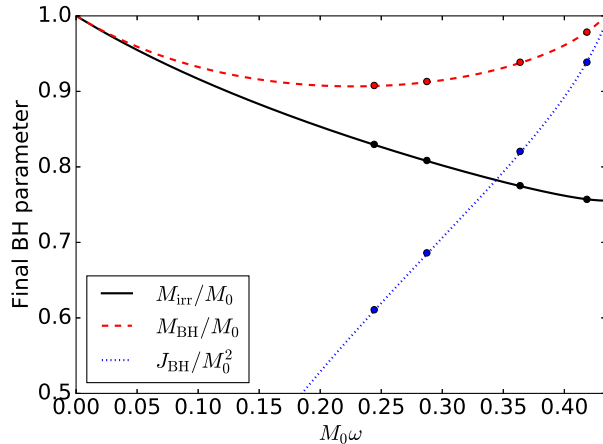


FIG. 3. The final BH irreducible mass, total mass, and angular momentum after saturation of the $m = 1$ super-radiant instability for a BH with $a = 0.99$ ($M_{\text{irr},0}/M_0 \approx 0.76$) initially. The lines show the prediction obtained with the assumption that the BH will lose energy and angular momentum in fixed proportion ω , until $\Omega_{\text{BH}} = \omega$, while the points show the measured values from the simulations.

sulting clouds are illustrated in Fig. 4 for two cases. Away from the BH, the Proca clouds have a roughly spherical energy density, falling off exponentially with distance from the BH. For the larger μ cases, the cloud is concentrated on much smaller scales near the BH.

As expected, given the close match between the energy and angular momentum lost by the BH and that gained by the Proca cloud, the radiation from both GWs and the Proca field is negligible (the dominant contribution of which comes from the other modes in the seed perturbation leading to initial radiation). The fact that we are considering a complex Proca field and restricting our study to axisymmetric spacetimes will suppress the gravitational radiation. We can estimate what the gravitational radiation would be for a single real Proca field by using the GW luminosity results from the test field limit [22] and scaling them using $P_{\text{GW}} \propto E^2$. This gives $P_{\text{GW}} \sim 6 \times 10^{-8}$, 2×10^{-7} , 6×10^{-7} , and 6×10^{-8} for the Proca field clouds at the end of the $\tilde{\mu} = 0.25, 0.3, 0.4$, and 0.5 simulations, respectively. This means that once the BH has spun down to below the superradiant regime, the Proca cloud will decay via GW emission on time scales of $\sim 10^5$ – $10^6 M_0$.

Our Proca field ansatz only allows exploration of the $m = 1$ mode instability. Higher m modes are also unstable, even after the BH has spun down to the point where the $m = 1$ becomes stable (ignoring

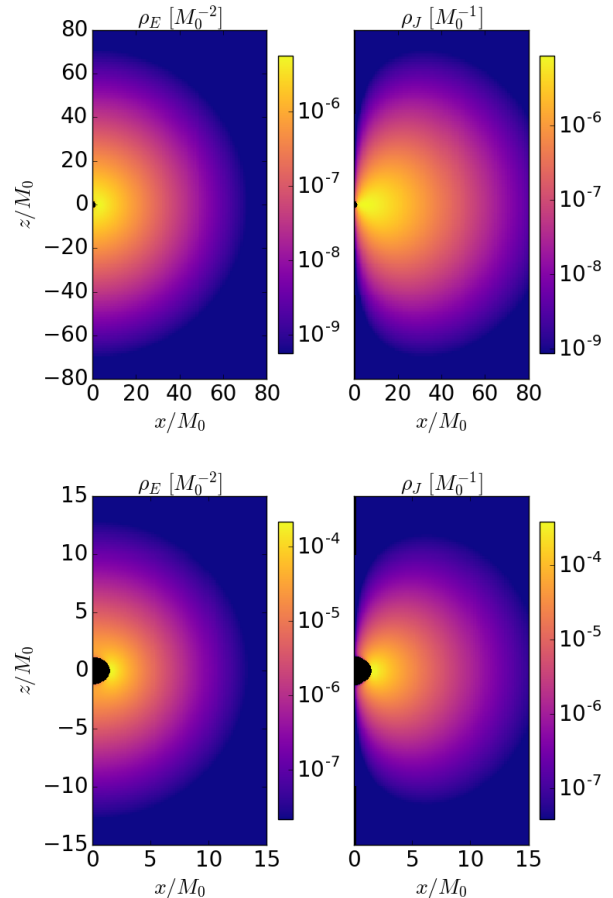


FIG. 4. The energy (left) and angular momentum density (right) of the Proca field in the final state with $\tilde{\mu} = 0.25$ (top) and $\tilde{\mu} = 0.5$ (bottom) for a slice containing the BH spin axis (the z axis) and perpendicular to the equatorial plane ($z = 0$); note the different scales for the two cases.

the Proca cloud). However, the grow rates become significantly longer with increasing m . For example, for $\tilde{\mu} = 0.5$ the $m = 2$ instability has a growth rate ~ 2000 times as long as the $m = 1$ mode [22], and the disparity is worse for smaller μ (with the relative growth rates scaling as μ^4).

Conclusion.—We have studied the growth and saturation of the superradiant instability of a massive vector field around a Kerr BH. We find that in all cases the instability efficiently extracts energy from the BH and then smoothly shuts off as the BH horizon frequency decreases to the threshold of instability. This contrasts with Ref. [2], where the energy extraction of a charged BH in a reflecting cavity was seen to overshoot in some cases; this could be due to the pres-

ence of multiple unstable modes [3]. We further find that at saturation essentially all the energy and angular momentum extracted from the BH has gone into forming a cloud of complex Proca “hair” with stationary energy density surrounding the BH. A family of stationary hairy BH solutions with this property and the same matter model was constructed in Ref. [28] which is plausibly the same as our end states; it would be interesting to investigate in detail how close these solutions are to what we find at saturation. In our case, the Proca clouds persist for the relatively short times we have extended the runs beyond saturation, though this is not adequate to comment on their long-term stability.

Acknowledgements.— We thank Asimina Arvanitaki, Masha Baryakhtar, Stephen Green, Robert Lasenby, Luis Lehner, Vasilis Paschalidis, Justin Ripley, Kent Yagi, and Huan Yang for stimulating discussions. This research was supported in part by Perimeter Institute for Theoretical Physics (WE), the National Science Foundation through Grant No. PHY-1607449 (FP), and the Simons Foundation (FP). Research at Perimeter Institute is supported by the Government of Canada through the Department of Innovation, Science and Economic Development Canada and by the Province of Ontario through the Ministry of Research, Innovation and Science. Simulations were run on the Perseus Cluster at Princeton University and the Sherlock Cluster at Stanford University.

[1] W. H. Press and S. A. Teukolsky, *Nature (London)* **238**, 211 (1972).
 [2] N. Sanchis-Gual, J. C. Degollado, P. J. Montero, J. A. Font, and C. Herdeiro, *Phys. Rev. Lett.* **116**, 141101 (2016), 1512.05358.
 [3] P. Bosch, S. R. Green, and L. Lehner, *Phys. Rev. Lett.* **116**, 141102 (2016), 1601.01384.
 [4] T. Damour, N. Deruelle, and R. Ruffini, *Lettere Al Nuovo Cimento Series 2* **15**, 257 (1976).
 [5] S. L. Detweiler, *Phys. Rev.* **D22**, 2323 (1980).
 [6] T. Zouros and D. Eardley, *Annals Phys.* **118**, 139 (1979).
 [7] A. Arvanitaki, S. Dimopoulos, S. Dubovsky, N. Kaloper, and J. March-Russell, *Phys. Rev.* **D81**, 123530 (2010), 0905.4720.
 [8] A. Arvanitaki and S. Dubovsky, *Phys. Rev.* **D83**, 044026 (2011), 1004.3558.
 [9] A. Arvanitaki, M. Baryakhtar, and X. Huang, *Phys. Rev.* **D91**, 084011 (2015), 1411.2263.
 [10] B. Holdom, *Phys. Lett.* **B166**, 196 (1986).
 [11] P. Pani, V. Cardoso, L. Gualtieri, E. Berti, and A. Ishibashi, *Phys. Rev.* **D86**, 104017 (2012),

1209.0773.
 [12] Virgo, LIGO Scientific, B. P. Abbott *et al.*, *Phys. Rev. Lett.* **116**, 061102 (2016), 1602.03837.
 [13] A. Arvanitaki, M. Baryakhtar, S. Dimopoulos, S. Dubovsky, and R. Lasenby, *Phys. Rev.* **D95**, 043001 (2017), 1604.03958.
 [14] M. Baryakhtar, R. Lasenby, and M. Teo, (2017), 1704.05081.
 [15] R. Brito, V. Cardoso, and P. Pani, editors, *Superradiance*, , Lecture Notes in Physics, Berlin Springer Verlag Vol. 906, 2015, 1501.06570.
 [16] W. E. East, F. M. Ramazanoğlu, and F. Pretorius, *Phys. Rev.* **D89**, 061503 (2014), 1312.4529.
 [17] O. Baake and O. Rinne, *Phys. Rev.* **D94**, 124016 (2016), 1610.08352.
 [18] P. Pani, V. Cardoso, L. Gualtieri, E. Berti, and A. Ishibashi, *Phys. Rev. Lett.* **109**, 131102 (2012), 1209.0465.
 [19] S. Endlich and R. Penco, *JHEP* **05**, 052 (2017), 1609.06723.
 [20] H. Witek, V. Cardoso, A. Ishibashi, and U. Sperhake, *Phys. Rev.* **D87**, 043513 (2013), 1212.0551.
 [21] M. Zilhão, H. Witek, and V. Cardoso, *Class. Quant. Grav.* **32**, 234003 (2015), 1505.00797.
 [22] W. E. East, (2017), 1705.01544.
 [23] W. E. East and F. Pretorius, *Phys. Rev.* **D87**, 101502 (2013), 1303.1540.
 [24] S. R. Dolan, *Phys. Rev.* **D76**, 084001 (2007), 0705.2880.
 [25] J. G. Rosa and S. R. Dolan, *Phys. Rev.* **D85**, 044043 (2012), 1110.4494.
 [26] S. R. Dolan, *Phys. Rev.* **D87**, 124026 (2013), 1212.1477.
 [27] R. Brito, V. Cardoso, and P. Pani, *Classical and Quantum Gravity* **32**, 134001 (2015), 1411.0686.
 [28] C. Herdeiro, E. Radu, and H. Runarsson, *Class. Quant. Grav.* **33**, 154001 (2016), 1603.02687.

Details of numerical methods

We employ fourth-order accurate finite difference methods to integrate the equations. For all of the simulations presented here we used a grid hierarchy with seven levels of mesh refinement, with 2:1 refinement ratio, centered on the BH. For the cases with $\tilde{\mu} = 0.4$ and 0.5, we performed the calculation at three different resolutions: the lowest has 96×192 points on each refinement level and a resolution of $dx/M_0 \approx 0.0256$ on the finest level. For the $\tilde{\mu} = 0.4$ case the medium and high resolutions have 4/3 and 2 times the low resolution, while for the $\tilde{\mu} = 0.5$ case the medium and high resolutions are 4/3 and 8/3 times the low resolution, respectively. In Fig. 5 we show resolution studies of the energy in the Proca field as a function of time. This data implies errors in measurements

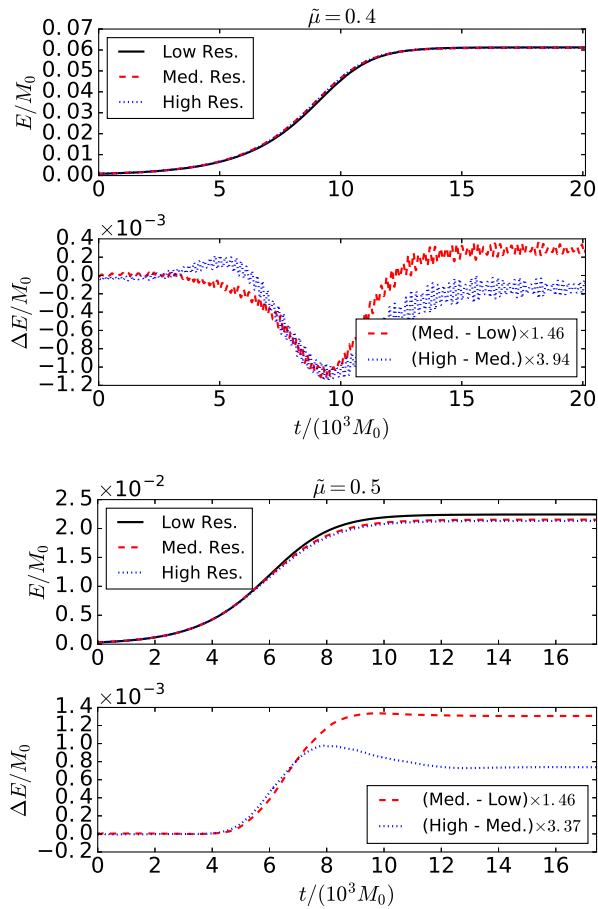


FIG. 5. The energy in the Proca field for simulations performed at three different resolutions, and the difference in this quantity with resolution, scaled assuming fourth-order convergence for $\tilde{\mu} = 0.4$ (top) and $\tilde{\mu} = 0.5$ (bottom).

of the energy of the field are a few percent at the lowest resolution, and are less than 1% for the high resolution runs throughout the simulation run time. We did not perform convergence studies for the two lower μ cases, as the much slower growth rates make

such studies prohibitively expensive. However, based on the convergence studies for the higher μ cases, we suspect errors in the lower μ runs — which have larger characteristic length scales — are still relatively small, at a few percent at most. In the main text all results are taken from the highest resolution data available.

Though we do not include the effect of the perturbation of the initial Proca field configuration on the initial BH spacetime, we have verified that it is so small as to introduce negligible error. This is illustrated in

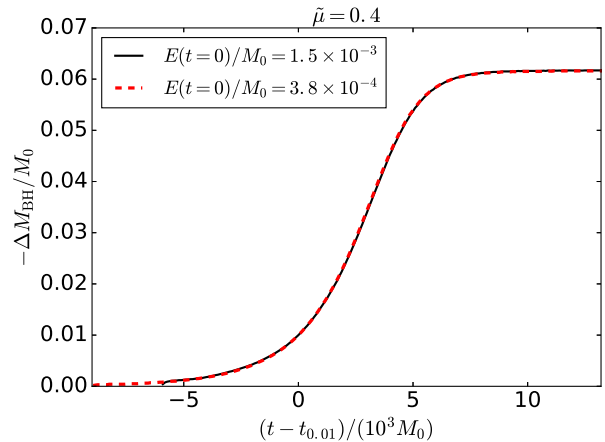


FIG. 6. The change in BH mass as a function of time for $\tilde{\mu} = 0.4$ for two cases: one where the initial Proca field configuration has $E(t=0)/M_0 = 1.5 \times 10^{-3}$, and one where the initial Proca field energy is four times smaller, but otherwise identical. A time shift has been applied so that the two curves align when $-\Delta M_{\text{BH}}/M_0 = 0.01$.

Fig. 6 where we show a comparison of the change in BH mass as a function of time for a simulation where we use an initial Proca field perturbation that is half the amplitude of the standard case, for $\tilde{\mu} = 0.4$. After applying a relative time shift (of $\approx 3000 M_0$, consistent with the test-field instability rate), the results from the two cases are indistinguishable on the scale of the figure.